Neurosci. Bull. September, 2022, 38(9):1041–1056
https://doi.org/10.1007/s12264-022-00892-z

www.neurosci.cn
www.springer.com/12264

ORIGINAL ARTICLE

Activation of Dopamine D2 Receptors Alleviates Neuronal Hyperexcitability in the Lateral Entorhinal Cortex *via* Inhibition of HCN Current in a Rat Model of Chronic Inflammatory Pain

Shi-Hao Gao[1,3] · Yong Tao[1] · Yang Zhu[1] · Hao Huang[1] · Lin-Lin Shen[2] · Chang-Yue Gao[1]

Received: 31 October 2021 / Accepted: 10 April 2022 / Published online: 15 June 2022

Abstract Functional changes in synaptic transmission from the lateral entorhinal cortex to the dentate gyrus (LEC-DG) are considered responsible for the chronification of pain. However, the underlying alterations in fan cells, which are the predominant neurons in the LEC that project to the DG, remain elusive. Here, we investigated possible mechanisms using a rat model of complete Freund's adjuvant (CFA)-induced inflammatory pain. We found a substantial increase in hyperpolarization-activated/cyclic nucleotide-gated currents (I_h), which led to the hyperexcitability of LEC fan cells of CFA slices. This phenomenon was attenuated in CFA slices by activating dopamine D2, but not D1, receptors. Chemogenetic activation of the ventral tegmental area -LEC projection had a D2 receptor-dependent analgesic effect. Intra-LEC microinjection of a D2 receptor agonist also suppressed CFA-induced behavioral hypersensitivity, and this effect was attenuated by pre-activation of the I_h. Our findings suggest that down-regulating the excitability of LEC fan cells through activation of the dopamine D2 receptor may be a strategy for treating chronic inflammatory pain.

Shi-Hao Gao and Yong Tao contributed equally to this work.

✉ Lin-Lin Shen
shlldyx@163.com

✉ Chang-Yue Gao
gaochangyue1990@163.com

[1] Department of Rehabilitation, Daping Hospital, Army Medical University, Chongqing 400042, China

[2] Department of Respiratory and Critical Care Medicine, Xinqiao Hospital, Army Medical University, Chongqing 400037, China

[3] Army 953 Hospital, Army Medical University, Shigatse 857000, China

Keywords Inflammatory pain · Lateral entorhinal cortex · Neuronal hyperexcitability · Dopamine D2 receptor · HCN current

Introduction

The lateral entorhinal cortex (LEC) not only mediates sensory and emotionally-salient inputs to the hippocampus but also plays an important role in chronic pain processing through interactions with the hippocampus [1–3]. Peripheral persistent nociception can amplify synaptic connections and transmission through the entorhinal cortex-dentate gyrus (EC-DG) synaptic pathway [4], mainly conveyed by excitatory glutamatergic connections. Bilateral LEC lesions have antinociceptive effects, raising the possibility that inhibition of LEC neuronal excitability also has an analgesic effect [5]. The most abundant neurons in layer II of the LEC that heavily innervate the DG with fibers forming the lateral perforant path belong to one type of stellate cell, namely, the fan cell [6]. Therefore, excitability changes in fan cells and their role in chronic pain attracted our attention.

Mounting evidence has shown that hyperpolarization-activated/cyclic nucleotide-gated ion channels (HCN channels) are densely expressed in cortical regions [7] and play a vital role in chronic pain [8–11]. Both the superficial layers of the medial and lateral EC express HCN channels [12]. In these regions, HCN channels are mainly expressed on the soma, and their activation generates an inward current, named I_h [12, 13]. The I_h is characteristic of stellate cells and fan cells, and it depolarizes the membrane potential of these cells to the firing threshold [14]. Considering this effect, we aimed to determine whether

the I_h is involved in excitability changes in fan cells in a chronic pain state.

Chronic pain patients suffer from low dopamine production and delivery in the mesolimbic system [15, 16], which delivers dopamine from the ventral tegmental area to neural structures such as the nucleus accumbens, prefrontal cortex, and anterior cingulate cortex [17]. Alterations in functional connections between the mesolimbic nodes and cortical regions play an important role in chronic pain [18–21]. Interestingly, inputs from midbrain dopamine neurons appear to specifically target clusters of excitatory cells located in the superficial layers of the entorhinal cortex [22]. Thus, we investigated whether the activation of dopaminergic receptors modulates the neuronal properties of fan cells in the LEC and exerts analgesic effects in a chronic pain state.

Therefore, we investigated alterations in the excitability of LEC fan cells and their I_h in a rat model of chronic inflammatory pain. Moreover, we studied whether activation of dopamine receptors changes neuronal excitability *via* modulating the I_h and alleviates behavioral hypersensitivity.

Materials and Methods

Experimental Animals

Male Sprague-Dawley rats [200–240 g for behavioral experiments; postnatal days 21–28 (P21–P28) for whole-cell recordings; Experimental Animal Centre of Army Medical University, Chongqing, China] were maintained on a 12-h light-dark cycle with free access to food and water at a constant room temperature of 25 °C–28 °C. All efforts were made to minimize suffering and to reduce the number of animals used to the minimum required for statistical accuracy. Every experimental procedure was executed in accordance with the National Institutes of Health Guide for the Care and Use of Laboratory Animals, approved by the Ethics Committee for Animal Research of the Army Medical University, and complied with relevant sections of the Animal Research: Reporting of *In Vivo* Experiments (ARRIVE) guidelines.

Induction of Inflammatory Pain

Inflammatory pain was induced as previously described [23–26]. Rats were randomized to the experimental or control group and anesthetized with urethane (U2500, Sigma-Aldrich, St. Louis, USA, 1 mg/kg, intraperitoneal); adequate anesthesia was ascertained by the lack of a corneal reflex. Then the rats received an intraplantar injection of 200 μL (20 μL for young rats) complete Freund's adjuvant (CFA; Sigma-Aldrich) in the plantar surface of the left hindpaw. Control rats were injected with the same volume of 0.9% saline. The rats were placed on a heating pad (RWD Life Science Co., Ltd., Shenzhen, China) after surgery to maintain the rectal temperature at 37°C until they were fully awake.

Brain Slice Preparation

For brain slice preparation, the brain of male Sprague-Dawley rats (P21 to P28), 3–7 days after saline or CFA injection, was quickly removed and submerged in a 0°C, pre-oxygenated (95% O_2, 5% CO_2) sucrose solution containing the following (in mmol/L): 220 sucrose, 10 D-glucose, 1.25 Na_2HPO_4, 26 $NaHCO_3$, 2.5 KCl, 6 $MgCl_2$, 1 $CaCl_2$. Horizontal slices (300 μm) containing the LEC and hippocampus (collected from the midline of the LEC to the dorsal side, as previously described [27]) were prepared using an oscillating tissue slicer (VT1000, Leica, Wetzlar, Germany) and transferred to an incubation chamber filled with artificial cerebrospinal fluid (aCSF), containing the following (in mmol/L): 119 NaCl, 2.5 KCl, 2.5 $CaCl_2$, 1.3 $MgCl_2{\cdot}6H_2O$, 1.25 $NaH_2PO_4{\cdot}2H_2O$, 26.2 $NaHCO_3$, 11 D-glucose, and aerated with a mixture of 95% O_2 and 5% CO_2 at 31 °C–33 °C before recording. After incubation for a minimum of 90 min, slices were transferred to a submersion-type recording chamber and perfused with constantly-aerated aCSF at 1 mL/min–2 mL/min.

Whole-Cell Clamp Recordings and Data Analysis

Whole-cell recordings in rat brain slice neurons were performed by investigators blinded to the slice preparation. Fan cells in LEC layer II (contralateral to the CFA injection site) were identified as previously described [27] and targeted for recording using an upright microscope equipped with Leica infrared-differential interference contrast optics, a 340 water-immersion objective, and a charge-coupled device camera. Recording electrodes made from 1.5-mm glass capillaries were pulled on a Flaming-Brown micropipette puller (P-97, Shutter Instrument, Novato, USA) and filled with an internal solution containing the following (in mmol/L): 145 potassium gluconate, 5 HEPES, 0.5 EGTA, 2 $MgCl_2$ and 5 K_2ATP (pH 7.2–7.4). With this solution, the recording electrodes had a resistance of 2.5 MΩ–6.0 MΩ. Liquid junction potentials were corrected arithmetically at the beginning of an experiment. Recordings were performed at 31 °C–33 °C. After gigaohm seal formation and patch rupture, series resistance was compensated 60%–80% and continually monitored throughout the experiment. In voltage-clamp experiments, capacitative transients were reduced by electronic capacitance compensation in the amplifier circuit. The current

clamp recordings were performed in bridge mode. Neurons were given at least 5 min to stabilize before data collection and were discarded if the series resistance increased by > 20%. The signals were low-pass-filtered at 5 kHz using a MultiClamp 700B amplifier (Molecular Devices, Sunnyvale, USA), digitized at 10 kHz (Digidata 1440A, Molecular Devices), and stored for offline analysis with pClamp9.2 software (Molecular Devices).

Data were analyzed using Clampfit (Molecular Devices), MatLab (MathWorks, Natick, USA), and Excel (Microsoft, Redmond, USA) [28]. The resting membrane potential was measured immediately after breaking into the cell. Input resistance was calculated from the linear portion of the current-voltage relationship generated in response to a series of 1000-ms current injections (− 300 to + 50 pA, in 50-pA steps). The fast afterhyperpolarization (fAHP) potential measurement was obtained when the mean first derivative of the trace reached 0.0 ± 0.5 V/s after each spike, using a 1-ms sliding average [29]. The action potential (AP) threshold was calculated as the point where the first derivative of the upsweep of the spike equaled 10 V/s. The AP half-width measurements were taken at half the AP peak amplitude relative to threshold. The voltage sag ratio was determined by the function [100 × (V_{ss}−−V_{min})/(V_{bsl}−V_{min})] at a negative current step that caused an approximately − 20 mV hyperpolarization of the membrane potential, where V_{bsl}, V_{ss}, and V_{min} indicate the baseline, steady-state, and minimum voltage, respectively. In this way, differences in input resistance were compensated [30].

Immunohistochemistry

Rats were anesthetized with urethane (1 mg/kg, intraperitoneal) and perfused through the ascending aorta with 300 mL 0.9% saline, followed by 300 mL of 4 °C 4% paraformaldehyde (PFA) in phosphate buffer (0.1 mol/L sodium phosphate, pH 7.4). Each brain was quickly removed and post-fixed for 24 h in phosphate-buffered 4% PFA at 4 °C. After dehydration in 30% phosphate-buffered sucrose solution, the brain area containing the LEC was horizontally cut at 25 μm on a cryostat (1900, Leica). The sections were first treated with 3% H_2O_2 for 10 min at room temperature, then incubated with 10% normal goat serum in 0.01 mol/L phosphate-buffered saline (PBS) for 1 h at 37 °C, and finally incubated with a mouse monoclonal HCN1 antibody (1:100; Abcam, Cambridge, USA), a rabbit D1R antibody (1:100; Abcam), or a rabbit D2R antibody (1:100; Abcam) at 4 °C overnight. After three 10-min PBS washes, the sections were incubated with a horseradish peroxidase-conjugated goat anti-mouse (or anti-rabbit) antibody (1:200; Zhongshan Goldenbridge Biotechnology, Beijing, China) for 1 h at 37°C, and then washed in PBS. Finally, sections were visualized with a diaminobenzidine tetrahydrochloride (DAB) chromogen (Zhongshan Goldenbridge Biotechnology) for 5 min. Immunohistochemistry images were obtained with a microscope (Leica, Wetzlar, Germany). Eight sections were extracted from a total of 40 sections (4-section intervals) of each brain for statistical analysis. The integrated optical density (IOD) was analyzed with Image-Pro Plus 6.0 (Media Cybernetics, Maryland, USA), and expressed as a fold increase compared with that of LEC superficial layers in the saline group.

Western Blot

Rats were euthanized with urethane (1 mg/kg, intraperitoneal). The LEC was quickly dissected on ice and homogenized in lysis buffer (12.5 μL/mg tissue) containing a mixture of protease inhibitors (Roche, Basle, Switzerland) and phenylmethylsulfonyl fluoride (PMSF; Sigma-Aldrich). Then, the samples were centrifuged at 10,000 r/min for 15 min at 4°C, and the supernatants were extracted for protein concentration measurements using a bicinchoninic acid (BCA) Protein Assay kit (ThermoFisher Scientific, Waltham, USA). Equal amounts of protein (50 μg) were loaded and separated on 8% Tris-Tricine SDS-PAGE gels. The resolved proteins were transferred onto polyvinylidene fluoride (PVDF) membranes (GE Healthcare Bio-Science, Pittsburgh, USA) and blocked in 5% nonfat milk (containing Tris-buffered saline, 0.1% Tween-20, pH 7.4) for 2 h at 37 °C. Then, the membranes were incubated overnight at 4 °C with a mouse monoclonal HCN1 antibody (1:1000; Abcam), a rabbit D1R antibody (1:1000 Abcam), a rabbit D2R antibody (1:1000; Abcam), or a rabbit β-actin antibody (1:1000; Zhongshan Goldenbridge Biotechnology), and were continuously incubated with a goat anti-mouse or anti-rabbit IgG conjugated with horseradish peroxidase (1:1000; Zhongshan Goldenbridge Biotechnology) at 37 °C for 1 h. Finally, signals were visualized using enhanced chemiluminescence (ECL, Pierce), and scanned using Odyssey scanner software (Li-COR Bioscience, Lincoln, USA). The density of specific bands was measured using Quantity One software (Bio-Rad, Hercules, USA). A square of the same size was drawn around each band to measure the density and the background near that band was subtracted. Protein levels were normalized against β-actin level and expressed as a fold increase compared with the saline group.

In Vivo Plasmid Adeno-associated Virus (AAV) Serotype 2/9 Injection

Rats were anesthetized with urethane (1 mg/kg, intraperitoneal) and placed into a digital stereotaxic device (RWD

Life Science Co., Ltd.) with bregma and lambda at the same horizontal level. A glass pipette (10–15 μm diameter tip) connected to an automated syringe pump (Stoelting Co., Los Angeles, USA) was inserted into the VTA (from bregma: anteroposterior, −5.04 mm; mediolateral, 0.5 mm; dorsoventral, −8.1 mm from the skull surface) according to the rat brain atlas. A volume of 0.25 μL of 1.75×10^{13} transducing units (TU) of AAV-dopamine transporter (DAT)-Gq-coupled human M3 muscarinic DREADD receptor (hM3Dq)-mCherry or 3.39×10^{13} TU of AAV-DAT-enhanced green fluorescent protein (EGFP) (Obio Technology Corp., Ltd., Shanghai, China) was injected over a 5-min period. The injection pipette was left in place for an additional 10 min to minimize efflux of the virus.

In Vivo Drug Application

Rats were anesthetized with urethane (1 mg/kg, intraperitoneal) and placed into a digital stereotaxic device (RWD Life Science Co., Ltd.) with bregma and lambda at the same horizontal level. A 30-gauge stainless-steel guide cannula with a 33-gauge stainless steel stylet plug (RWD Life Science Co., Ltd.) was inserted in the LEC (from bregma: anteroposterior, −7.8 mm; mediolateral, 6.2 mm; dorsoventral, −6.8 mm) based on the rat brain atlas [31, 32], 0.5 mm above the injection site. The rats were given 1 week to recover from cannula implantation. Microinjections were performed on awake rats through the 33-gauge cannula linked to a syringe pump (Stoelting Co.) by a long flexible tube. The injection cannula was extended 0.5 mm beyond the tip of the guide cannula and a volume of 0.5 μL of clozapine-N-oxide (CNO; Sigma-Aldrich), quinpirole, 8-Br-cAMP, SCH23390, sulpiride, or aCSF was injected over a 5-min period. In some cases, cholera toxin subunit B (Alexa Fluor 594, dissolved at 1 μg/μL; Thermo-Fisher Scientific) was added to the injection solution to verify the diffusion range. The injection cannula was left in place for an additional 5 min and quickly replaced by the stylet plug to minimize the efflux of the drug or aCSF. The rats were allowed to recover for 15 min before the behavioral experiment.

Behavioral Measurements

The tests of pain threshold were conducted on the hindpaws as described previously [33] and the experiments were blinded to drug application. All of the rats were pre-exposed to the experimental chamber for 3 h per day for 3 days for habituation before the behavioral tests. Thermal hyperalgesia was assessed using the Hargreaves test [34]. Each rat was individually placed in a Plexiglas chamber on a 3-mm thick glass platform, under which a radiant heat source (IITC Life Science, Pittsburgh, USA) was directed at the proximal half of the hindpaw plantar surface and created a 4 mm × 5 mm intense light spot on the paw. The distance between the top of the heat source and the glass platform was 2.5 cm and the power of the heat source was set to 10 Watts. The heat source was turned off immediately when the rat briskly lifted the foot, allowing the measurement of the paw withdrawal thermal latency as the threshold of thermal sensitivity. Each hindpaw was tested five times at 2-min intervals, and a 60-s cutoff was used to prevent tissue damage in the absence of a response.

Mechanical allodynia was measured using a calibrated series of von Frey hairs (vFh) with bending forces in the range of 0.3 g–60.3 g. Tests were initiated with a 4.10 g vFh, the middle of the filament series. The filament was applied to the plantar surface of the hindpaw with sufficient force to bend it for 2 s. A positive paw withdrawal response was recorded if the hindpaw was briskly lifted and completely removed from the platform. The 50% paw withdrawal mechanical threshold was determined by the up-down method [35].

Drugs

All of the reagents were from Sigma-Aldrich except for (±)-1-Phenyl-2,3,4,5-tetrahydro-(1*H*)-3-benzazepine-7,8-diol hydrobromide (SKF38393), (4a*R*-trans)-4,4a,5,6,7,8,8a,9-Octahydro-5-propyl-1*H*-pyrazolo[3,4-*g*]quinoline hydrochloride (quinpirole), and ZD7288, which were from Tocris Bioscience (Bristol, UK). During whole-cell recording, all drugs were dissolved in their solvents as stock solutions and were applied by switching the perfusion from aCSF to a solution containing the desired drug at an appropriate concentration. For *in vivo* drug application, each specified stock solution was diluted by aCSF to the desired concentration before microinjection. The vehicle solution was aCSF. All of the stock solutions were stored in tightly-sealed vials at –20 °C and used within 1 month.

Statistical Analysis

No statistical analysis was used to predetermine the sample size, but our sample sizes were based on several previous reports and our previous publications. All quantitative values were normally distributed and are expressed as the mean ± SEM. All comparisons between two groups were analyzed using Student's unpaired *t*-tests, with the exception of the comparison of I_h amplitude and onset frequency before and after application of ZD7288 that were assessed using Student's paired *t*-tests. The comparison of cumulative probability distributions of the interspike intervals (ISIs) was analyzed using the Kolmogorov-Smirnov (K-S) test. The fAHP, current-voltage (*I-V*) curve of I_h, and pain

thresholds were analyzed using the two-way repeated-measures analysis of variance (ANOVA) followed by *post hoc* Bonferroni multiple comparison tests. One-way repeated-measures ANOVA followed by *post hoc* Bonferroni multiple comparison tests was used to compare the I_h amplitude and onset frequency before, during, and after drug application. The Friedman M test followed by the Dunn-Bonferroni *post hoc* test was also used in cases when equal variance was not assumed. Statistical comparisons were made using SPSS version 19 software (SPSS Inc., Chicago, USA). In all cases, $P < 0.05$ (two-tailed test) was considered to be statistically significant; "*n*" refers to the number of cells recorded unless stated otherwise.

Results

Inflammatory Pain-induced Alterations in Cellular Excitability of LEC Fan Cells

To establish the inflammatory pain model, rats received an intraplantar injection of CFA, which caused thermal hyperalgesia and mechanical allodynia specifically in the injured hindpaw, consistent with the previous description of this model (thermal latency: two-way repeated-measures ANOVA: main effect of group $F_{(3,22)} = 5.538$, $P = 0.005$; saline group $n = 6$ rats, CFA group $n = 7$ rats; mechanical threshold: two-way repeated-measures ANOVA: main effect of group $F_{(3,20)} = 79.576$, $P = 0.000$; all groups $n = 6$ rats; Fig. 1). We first evaluated the passive membrane properties of LEC fan cells on days 3–7 after CFA injection, and cells from rats that received intraplantar saline injection were used as controls. The results showed that the resting membrane potential, membrane capacitance, input resistance, and rheobase of LEC fan cells were comparable between the CFA and saline groups (Table 1). Then we investigated the excitability of fan cells by characterizing the AP firing patterns. Spontaneous firing for 1 min was recorded after holding the membrane potential at a slightly depolarized level (−55 mV; Fig. 2A). We found that the mean number of APs in fan cells was much higher in the CFA group than in the saline group (unpaired Student's *t*-test: $P = 0.032$; saline group $n = 9$, CFA group $n = 10$; Fig. 2B). The mean ISI was significantly shorter in the CFA group than in the saline group (unpaired Student's *t*-test: $P = 0.048$; saline group $n = 9$, CFA group $n = 10$; Fig. 2C). Moreover, the cumulative probability distribution of the ISIs in the CFA group was markedly left-shifted compared with that in the saline group (K-S test: $P < 0.05$; Fig. 2D), which also reflected an increase in firing frequency.

The firing properties were more precisely analyzed by applying depolarizing currents (100–300 pA, in 100-pA steps) for 500 ms (Fig. 2E). There were no significant differences in the mean number of APs elicited by each of these stimuli between fan cells from the CFA and saline groups during the entire 500 ms (AP number: 100 pA: saline 6.22 ± 0.64, $n = 9$, CFA 7.00 ± 0.68, $n = 10$; 200 pA: saline 9.63 ± 0.53, $n = 8$, CFA 10.56 ± 0.57, $n = 9$; 300 pA: saline 11.33 ± 0.83, $n = 6$, CFA 12.38 ± 0.70, $n = 8$; unpaired Student's *t*-test: 100 pA $P = 0.421$, 200 pA $P = 0.282$, 300 pA $P = 0.424$). However, measurements of the instantaneous firing frequency associated with the first 6–9 ISIs during these current steps showed a significantly higher frequency at onset (f_o) in the CFA group than in the saline group (unpaired Student's *t*-test: 100 pA: $P = 0.007$, 200 pA: $P = 0.006$, 300 pA: $P = 0.001$; all groups: saline $n = 9$, CFA $n = 10$; Fig. 2F), while the frequency at steady-state (f_{ss}) was almost identical in both groups during each depolarizing current step (unpaired Student's *t*-test: 100 pA: $P = 0.721$, saline $n = 6$, CFA $n = 8$; 200 pA: $P = 0.977$, saline $n = 6$, CFA $n = 9$; 300 pA: $P = 0.955$, saline $n = 5$, CFA $n = 8$; Fig. 2F). Thus, the LEC fan cells in the CFA group showed an initially higher excitability during physiologically pertinent depolarizing stimuli.

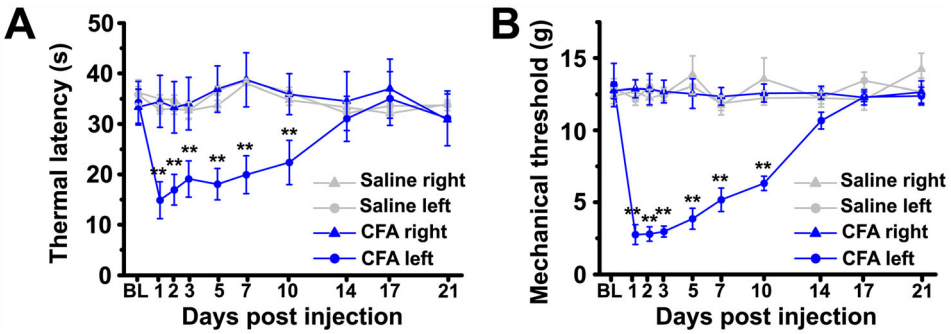

Fig. 1 CFA evokes thermal hyperalgesia and mechanical allodynia in the injured hind paw. **A** Progression of thermal latency following intraplantar CFA or saline injection. **B** Progression of mechanical threshold following intraplantar CFA or saline injection. BL, baseline; saline right, the right hindpaw of rats received a saline injection. $^{**}P < 0.01$.

Table 1 Passive membrane properties of LEC fan cells do not change after CFA injection

	RMP (mV)	C_m (pF)	R_N (MΩ)	Rheobase (pA)
Saline (n = 15)	− 58.75 ± 1.38	111.34 ± 8.79	131.84 ± 5.09	36.67 ± 2.89
CFA (n = 16)	− 55.99 ± 1.95	99.60 ± 10.77	112.21 ± 10.28	31.00 ± 3.43
P	0.263	0.409	0.104	0.341

RMP, resting membrane potential, C_m, membrane capacitance, R_N, input resistance, and rheobase of LEC fan cells in rats receiving intraplantar saline or CFA injection. Unpaired Student's t-test. Data are shown as the mean ± SEM.

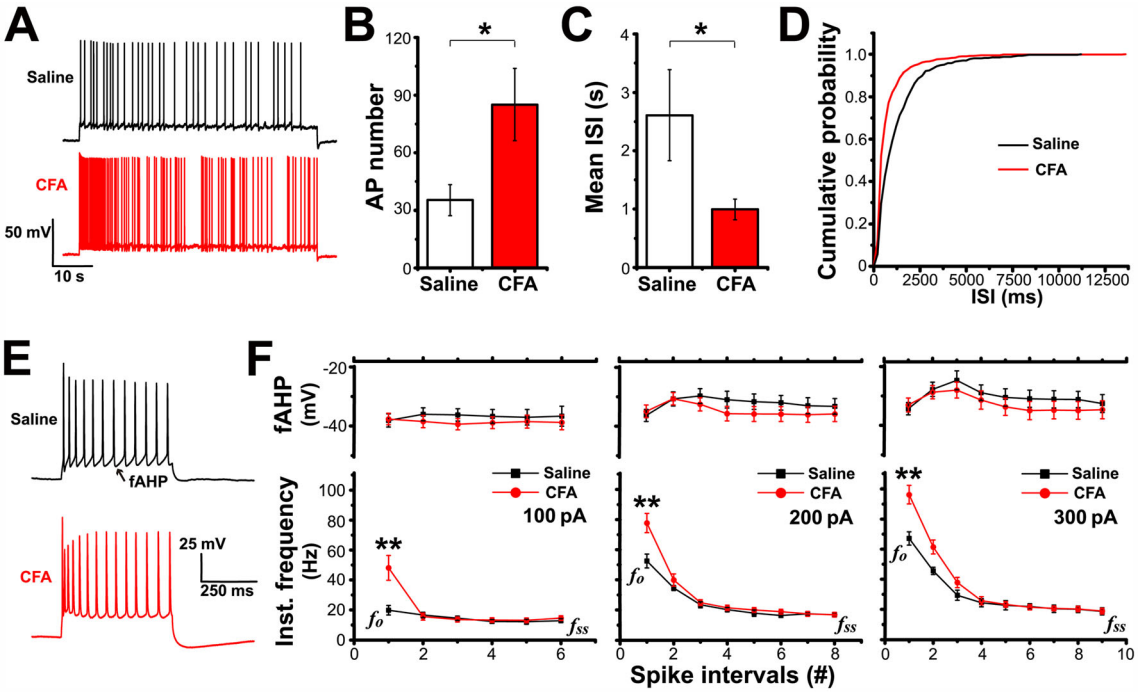

Fig. 2 Firing property of LEC fan cells is changed after CFA injection. **A** Representative traces showing the firing response of LEC fan cells to a 1-min rheobase stimulus. **B, C** Action potential (AP) numbers and mean interspike intervals (ISI) of LEC fan cells elicited by a 1-min rheobase stimulus. **D** CFA injection induces a marked leftward shift of the ISI cumulative distribution curve. **E** Representative traces showing the firing responses of LEC fan cells to a depolarizing current stimulus (+ 300 pA, 500 ms). **F** Fast afterhyperpolarization potential (fAHP, upper panel) and instantaneous frequency (Inst., lower panel) of AP firing in response to 100, 200, or 300 pA current injection. Data are from the first 6–9 spike intervals; #, number of spike intervals. f_o, onset frequency; f_{ss}, steady-state frequency. $^*P < 0.05$, $^{**}P < 0.01$.

Although fAHP is known to play an important role in determining the spike frequency during burst firing [36], we found no difference in fAHP between the two groups (two-way repeated-measures ANOVA: 100 pA: main effect of group $F_{(1,9)}$ = 0.155, P = 0.703, saline group n = 5, CFA group n = 6; 200 pA: main effect of group $F_{(1,14)}$ = 0.251, P = 0.624, saline group n = 7, CFA group n = 9; 300 pA: main effect of group $F_{(1,11)}$ = 0.042, P = 0.842, saline group n = 5, CFA group n = 8; Fig. 2F). In addition, the shape of the first AP elicited by the 200-pA depolarizing current was analyzed as an example to investigate the involvement of Na^+ channels in setting the firing frequency. As shown in Table 2, the threshold, peak, half-width, and max dV/dt values were similar in cells from the saline and CFA groups, suggesting that Na^+ channels are not the main cause of the higher onset frequency found in the CFA rats.

I_h of LEC Fan Cells is Up-regulated After CFA Injection

Given that I_h is a characteristic of fan cells in the superficial layer of the LEC and contributes to the depolarizing property of these cells, we then aimed to determine whether there was any difference in the I_h between the CFA and saline groups. The voltage sag ratio, which reflects the degree of I_h-induced membrane depolarization, was significantly higher in the CFA group than in the saline group (unpaired Student's t-test: P = 0.040; saline group n = 15, CFA group n = 16; Fig. 3A, B). I_h was directly

Table 2 Action potential waveforms of LEC fan cells are unaltered after CFA injection

	Threshold (mV)	Peak (mV)	Half-width (ms)	Max d*V*/d*t* (V/s)
Saline (n = 9)	− 32.33 ± 1.38	46.68 ± 1.05	2.11 ± 0.09	161.61 ± 11.47
CFA (n = 10)	− 35.25 ± 1.72	49.82 ± 1.35	2.04 ± 0.12	175.29 ± 13.92
P	0.211	0.088	0.643	0.464

Action potential threshold, peak potential, half-width, and maximum rate of rise of LEC fan cells in rats receiving intraplantar saline or CFA injection. Data are from the first AP elicited by a 200-pA depolarizing stimulus (500 ms in duration). Unpaired Student's *t*-test. Data are shown as the mean ± SEM.

induced by applying a series of hyperpolarizing voltage steps (−60 to −120 mV, in 10-mV steps) followed by a voltage jump to −120 mV to obtain full activation (Fig. 3C). We noted that the *I-V* curve of the I_h was prominently down-shifted after CFA injection, indicating an increase in I_h amplitude at almost all hyperpolarized voltage steps (two-way repeated-measures ANOVA: main effect of group $F_{(1,29)} = 11.346$, $P = 0.002$; saline group n = 15, CFA group n = 16; Fig. 3D). Measurements of the current density further confirmed that I_h was up-regulated after CFA injection (unpaired Student's *t*-test: $P = 0.003$; saline group n = 15, CFA group n = 16; Fig. 3E).

We next investigated the causal relationship between the I_h and hyperexcitability of LEC fan cells. Bath application of 10 μmol/L ZD7288 (a selective HCN channel blocker) almost completely abolished the I_h in fan cells (paired Student's *t*-test: $P = 0.000$; $n = 8$; Fig. 3F). In this condition, we found that the onset frequency of firing elicited by a 200-pA stimulus was down-regulated in the CFA group to a level identical to that in the saline group (paired Student's *t*-test: $P = 0.001$; $n = 8$; Fig. 3G). These results suggested that the increased onset frequency in fan cells after CFA injection probably resulted from the up-regulation of the I_h.

Among the 4 subtypes of HCN channels, the HCN1 channel is the most dominant subtype in the cerebral cortex. Analysis of the relative IOD levels of immunohistochemistry (IHC) staining showed that there was no difference in the HCN1 expression level between the CFA and saline groups (unpaired Student's *t*-test: $P = 0.818$; saline group n = 5 rats, CFA group n = 6 rats; Fig. 3H, I). Similarly, Western blot analysis revealed no significant alteration of the HCN1 protein level after CFA injection (unpaired Student's *t*-test: $P = 0.077$; all group n = 6 rats; Fig. 3 J).

Dopamine D2 Receptor (D2R) Activation Attenuates the I_h and Hyperexcitability of LEC Fan Cells in Inflammatory Pain

Given the causal relation of I_h up-regulation and increased activity of fan cells, and the unchanged HCN1 expression level after CFA injection, we wondered whether there was any pharmacological method to down-regulate the I_h. The superficial layer of the LEC is highly innervated by fibers releasing neuromodulators. Among them, dopamine could be of potential relevance since the mesolimbic dopamine system has been shown to be a potential target for pain treatment [17]. There are two kinds of dopamine receptor families, the D1-like and D2-like families [37, 38], both of which modulate the cytosolic levels of cAMP by changing the activity of adenylate cyclase. Therefore, given that the I_h can be modulated by the levels of cAMP [39], we aimed to explore whether the activation of dopamine receptors attenuates the I_h in fan cells.

We found that activation of the dopamine D1R by bath application of 30 μmol/L SKF38393 dramatically increased the I_h amplitude in fan cells in the CFA group (one-way repeated measures ANOVA: $F_{(2)} = 18.899$, $P = 0.000$; $n = 8$; Fig. 4A, B). This was accompanied by an increase in the onset frequency during the burst elicited by a 200-pA depolarizing stimulus (Friedman M test: $\chi^2 = 14.250$, $df = 2$, $P = 0.001$; $n = 8$; Fig. 4C, D). The effects of SKF38393 were eliminated after a 10-min washout. In contrast, activation of the D2R by bath application of 10 μmol/L quinpirole prominently decreased the I_h amplitude in the fan cells from the CFA group (one-way repeated measures ANOVA: $F_{(2)} = 52.964$, $P = 0.000$; $n = 8$; Fig. 4E, F). Simultaneously, we found that the onset frequency of fan cells was also significantly decreased by quinpirole (one-way repeated measures ANOVA: $F_{(2)} = 16.501$, $P = 0.000$; $n = 8$; Fig. 4G, H). Thus, activation of the dopamine D2R, but not D1R, could be a potential therapeutic strategy.

We therefore explored whether activation of dopamine D2Rs act on the I_h to modulate the onset frequency of LEC fan cells. In the presence of 10 μmol/L ZD7288 (ZD), a selective HCN channel blocker that nearly completely abolished the I_h and significantly decreased the onset frequency, quinpirole (quin) no longer had an additional effect (for I_h analysis: Friedman M test: $\chi^2 = 9.333$, $df = 2$, $P = 0.009$; ZD *vs* ZD + quin: Dunn-Bonferroni *post hoc* test: $P = 0.778$; $n = 6$; Fig. 5A, B; for f_o analysis: one-way repeated-measures ANOVA: $F_{(2)} = 35.120$, $P = 0.000$; ZD *vs* ZD + quin: *post hoc* Bonferroni test: $P = 0.995$; $n = 6$; Fig. 5C, D). Similarly, in the presence of 1 mmol/L 8-Br-

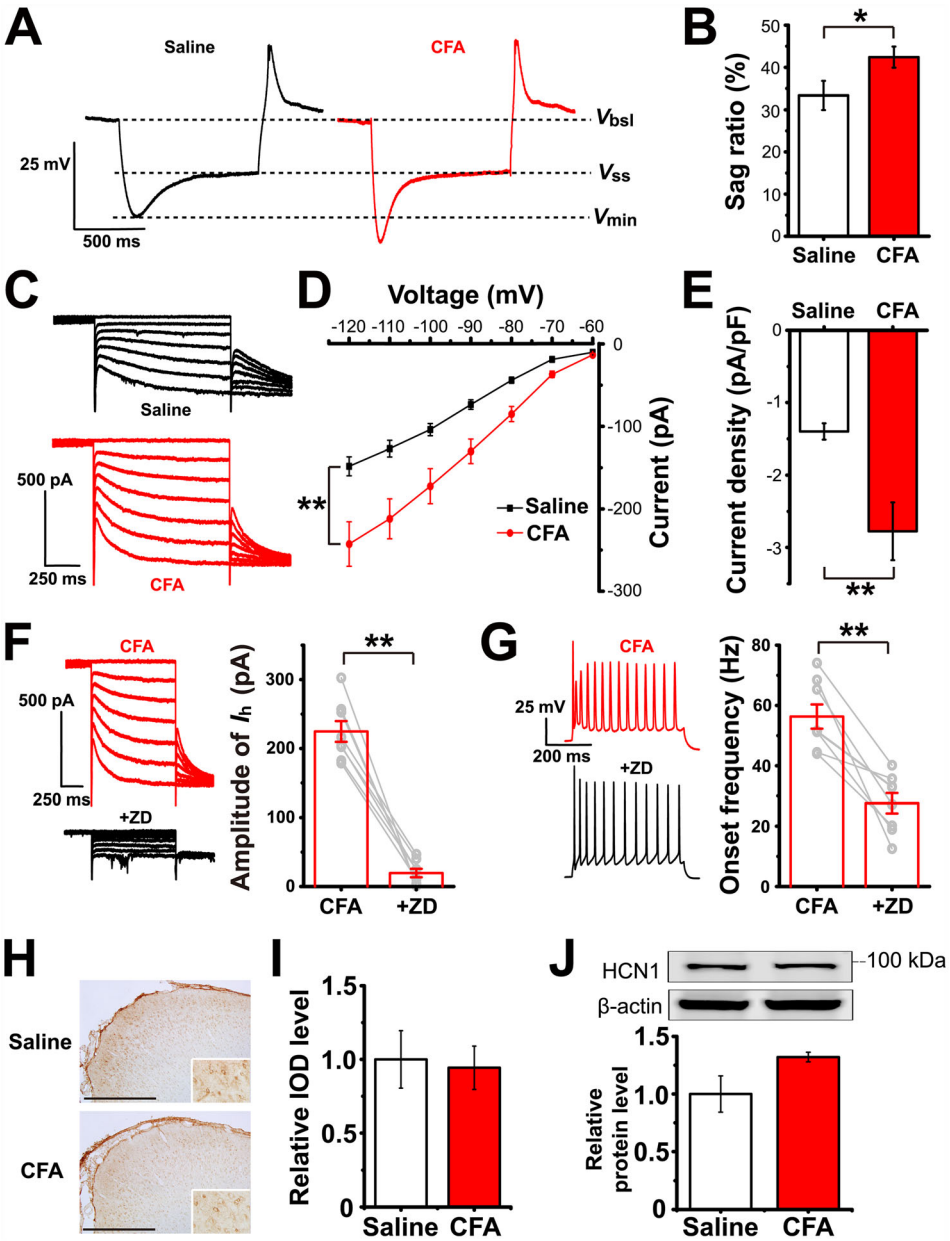

Fig. 3 I_h of LEC fan cells is up-regulated after CFA injection. **A** Representative traces of voltage sag induced by a current step that causes an approximately − 20 mV hyperpolarization at the steady state. V_{bsl}, baseline voltage; V_{ss}, steady-state voltage; V_{min}, minimum voltage. **B** Voltage sag ratios in the saline and CFA groups. **C** Representative traces of I_h induced by applying 1-s hyperpolarizing voltage steps from − 60 to − 120 mV (in 10-mV steps). **D** Current-voltage relationships of I_h in LEC fan cells from the saline and CFA groups. **E** I_h density at − 120 mV. **F** I_h is blocked after bath application of 10 μmol/L ZD7288 in LEC fan cells of the CFA group. **G** Onset frequency of the fan cells in **F** is significantly reduced after bath application of 10 μmol/L ZD7288. Left panel, representative traces showing that the onset frequency is measured between the 1st and 2nd AP elicited by a 200-pA depolarizing stimulus. **H** Representative immunohistochemistry images showing the expression pattern of HCN1 in the LEC (scale bar, 500 μm). Inserts, magnified images of HCN1-positive cells. **I** Relative IOD levels of HCN1 in the LEC are almost identical in the saline and CFA groups, as shown by immunohistochemistry. The IOD levels are expressed as a fold increase compared with the mean of the saline group in this and the following figures in this format. **J** Western blots and analysis of HCN1 expression levels in the saline and CFA groups. The relative protein levels are normalized as a ratio of β-actin levels and expressed as fold increase compared with the mean of the saline group in all Western blot figures. $^*P < 0.05$, $^{**}P < 0.01$.

cAMP, an HCN channel agonist that further increased the I_h amplitude and onset frequency, quinpirole did not down-regulate the onset frequency (for I_h analysis: one-way repeated-measures ANOVA: $F_{(2)} = 12.387$, $P = 0.002$; cAMP *vs* cAMP + quin: *post hoc* Bonferroni test: $P = 1.000$; $n = 6$; Fig. 5E, F; for f_o analysis: one-way repeated-

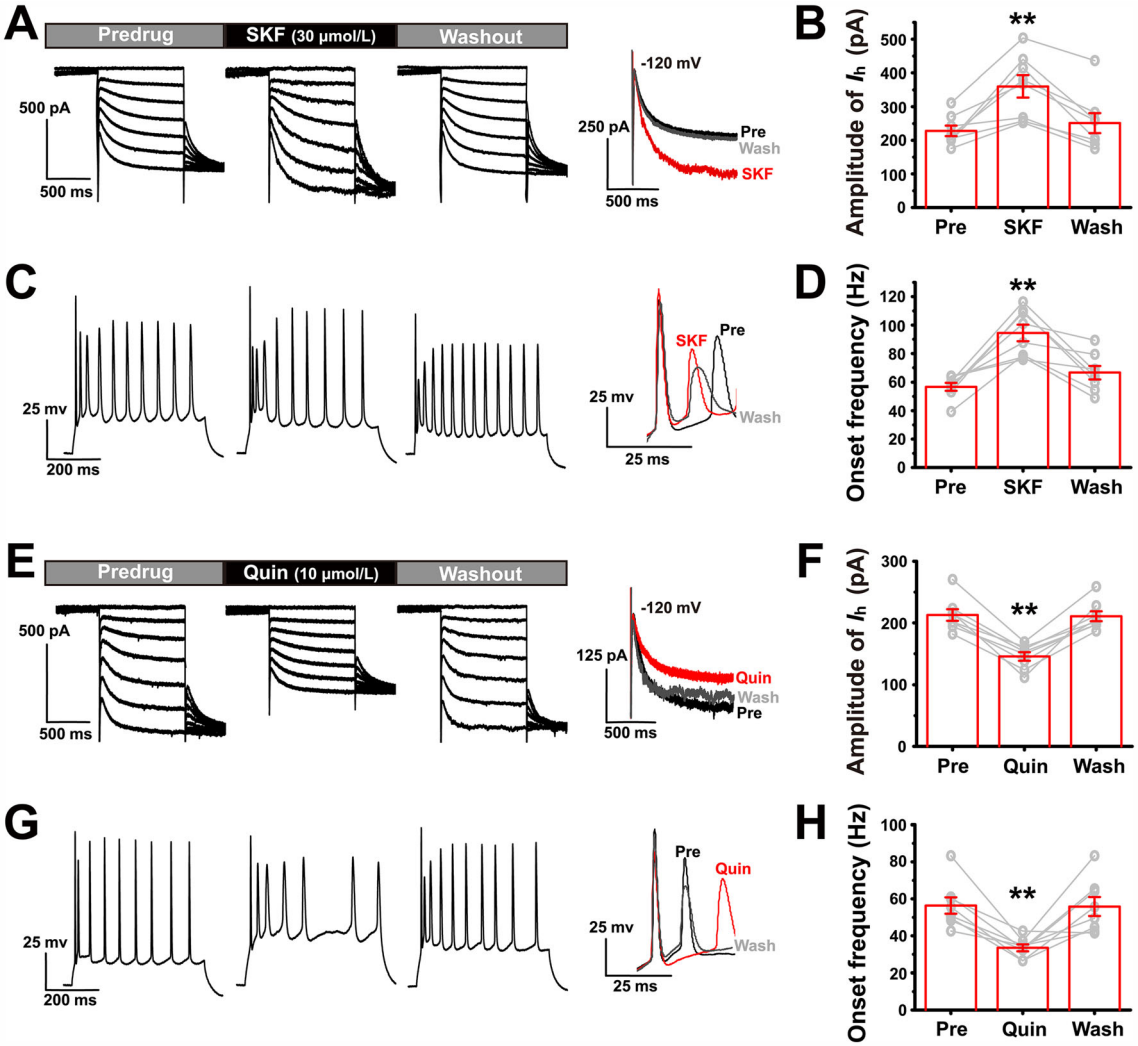

Fig. 4 Effects of dopamine D1 and D2 receptor agonists on I_h and onset frequency of LEC fan cells in the CFA group. **A, E** Changes in I_h of LEC fan cells during bath application of 30 μmol/L SKF38393 or 10 μmol/L quinpirole. Right panel, amplified current amplitude at − 120 mV. **C, G** Changes in the firing of LEC fan cells during bath application of 30 μmol/L SKF38393 or 10 μmol/L quinpirole. Right panel, amplified onset frequency. Spikes are elicited by a 200-pA depolarizing stimulus (500 ms in duration). **B** I_h amplitude in pre-drug, SKF38393, and washout in fan cells at − 120 mV. ** *vs* pre. For this and the following figures in this format, the grey circles represent data from individual cells. **D** Onset frequency in pre-drug, SKF38393, and washout in fan cells. ** *vs* pre. **F** I_h amplitude in pre-drug, quinpirole, and washout in fan cells at − 120 mV. ** *vs* pre. **H** Onset frequency in pre-drug, quinpirole, and washout in fan cells. ** *vs* pre. $^{**}P < 0.01$.

measures ANOVA: $F_{(2)} = 17.086$, $P = 0.001$; cAMP *vs* cAMP + quin: *post hoc* Bonferroni test: $P = 1.000$; $n = 6$; Fig. 5G, H). These results indicated that D2Rs probably modulate the onset frequency of fan cells by acting on the I_h.

Adenylate Cyclase (AC) Mediates the Regulatory Effect of the D2R on I_h

It has been shown that the D2R inhibits AC, while the AC usually activates I_h. Therefore, we also aimed to confirm that the modulation of the I_h by the dopamine D2R is mediated *via* inhibition of AC activity. We first confirmed that inhibition of AC directly down-regulates I_h in CFA brain slices. The results showed that bath application of an AC inhibitor (SQ22536, 10 μmol/L) significantly down-regulated the I_h amplitude (one-way repeated measures ANOVA: $F_{(2)} = 10.552$, $P = 0.003$; $n = 6$; Fig. 6A, C), indicating that under inflammatory pain conditions, the AC is tonically activated to maintain a large I_h level. Thus, when the AC was fully activated by incubating the CFA brain slice with 10 μmol/L forskolin (FSK), the I_h of fan cells was further increased. However, the subsequent bath application of 10 μmol/L quinpirole failed to down-regulate the I_h (Friedman M test: $\chi^2 = 9.000$, $df = 2$, $P = 0.011$; FSK *vs* FSK + quin: Dunn-Bonferroni *post hoc* test:

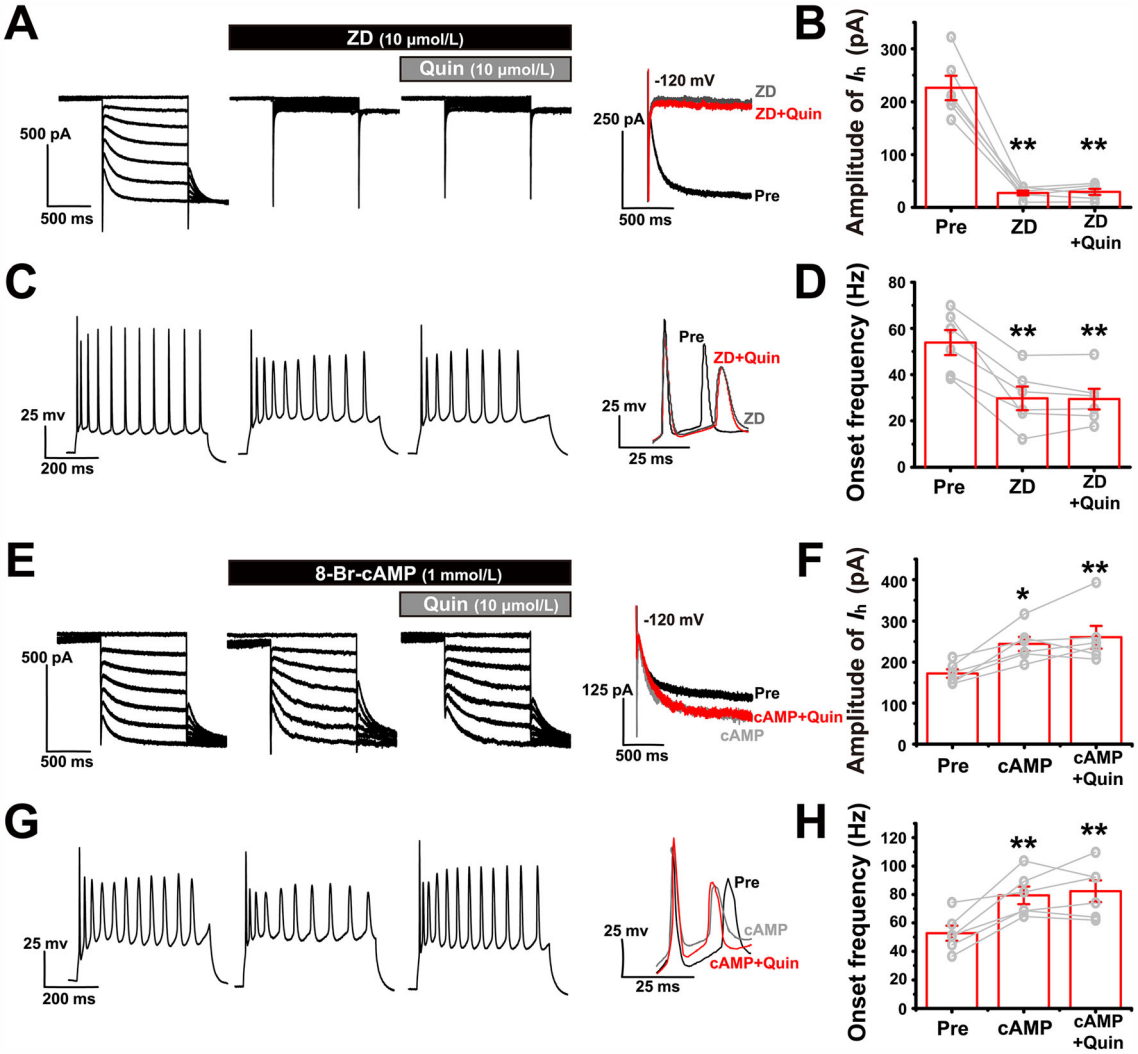

Fig. 5 D2R interacts with the HCN channel to modulate the onset frequency. **A** I_h of fan cells is almost completely blocked by 10 μmol/L ZD7288 and subsequent additional application of 10 μmol/L quinpirole fails to modulate it. **C** The onset frequency of fan cells decreases during bath application of 10 μmol/L ZD7288 and subsequent additional application of 10 μmol/L quinpirole has no effect. **B, D** I_h amplitude at −120 mV and onset frequency in pre-drug, ZD7288, and ZD7288 + quinpirole. ** *vs* pre. **E** I_h of fan cells is up-regulated by 1 mmol/L 8-Br-cAMP (cAMP) and subsequent additional application of 10 μmol/L quinpirole fails to decrease it. **G** The onset frequency of fan cells increases during bath application of 1 mmol/L 8-Br-cAMP and subsequent additional application of 10 μmol/L quinpirole has no effect. **F, H** I_h amplitude at −120 mV and onset frequency in pre-drug, 8-Br-cAMP, and 8-Br-cAMP + quinpirole. *, ** *vs* pre. $^*P < 0.05$, $^{**}P < 0.01$.

$P = 0.739$; $n = 6$; Fig. 6B, D). These results indicated that in inflammatory pain the activation of D2Rs down-regulates the I_h *via* inhibition of AC.

Activation of Dopamine D2Rs in the Superficial Layer of the LEC Alleviates the Behavioral Hypersensitivity Associated with Inflammatory Pain

We compared the D1R and D2R expression levels between saline and CFA groups with immunostaining (Fig. 7A, C). The results showed that expression levels of these receptors were not significantly changed (unpaired Student's *t*-test: D1R $P = 0.780$, D2R $P = 0.401$; all groups $n = 6$ rats; Fig. 7B, D). The Western blot analysis also showed no difference in the expression of these proteins between the saline and CFA groups (unpaired Student's *t*-test: D1R $P = 0.407$, D2R $P = 0.616$; all groups $n = 6$ rats; Fig. 7E, F). However, in CFA rats the activity of dopaminergic neurons is reduced according to previous reports [40], so that the dopamine concentration at axon terminals is probably changed to exert an altered modulatory effect on receptors. For this reason, we performed chemogenetic experiments to activate the projection from VTA to LEC, and determined whether there is any analgesic effect.

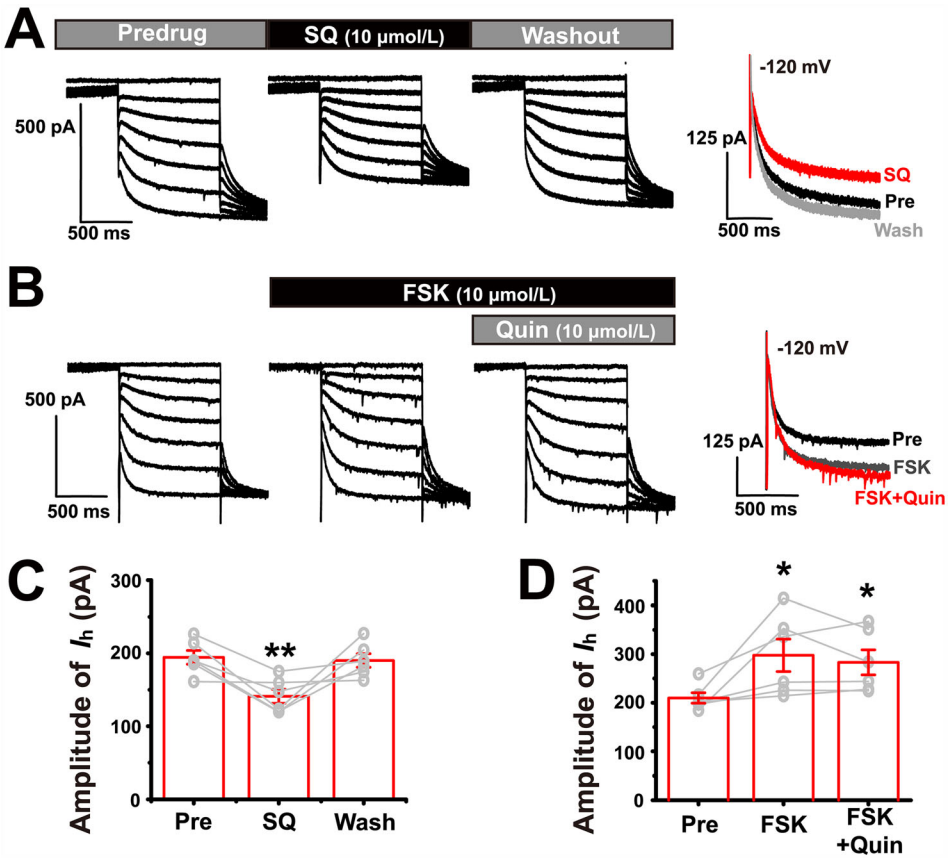

Fig. 6 AC mediates the effect of D2R on I_h. **A** I_h of fan cells is significantly down-regulated by 10 μmol/L SQ22536. **B** I_h of fan cells is up-regulated by 10 μmol/L forskolin (FSK) and subsequent additional application of 10 μmol/L quinpirole fails to decrease it. **C** I_h amplitude at −120 mV in pre-drug, SQ22536, and washout. ** *vs* pre. **D** I_h amplitude at −120 mV in pre-drug, forskolin, and forskolin + quinpirole. * *vs* pre. $^*P < 0.05$, $^{**}P < 0.01$.

We injected AAV-DAT-hM3Dq-mcherry into the VTA, inserted a cannula, and injected CNO (3 μmol/L) into the superficial LEC to specifically activate the VTA dopaminergic projection terminals in the LEC (Fig. 8A). AAV-DAT-EGFP and vehicle were injected as controls, as previously described [33]. The results showed a clear analgesic effect of activating the VTA-LEC projection, reflected by the elevated thermal latency (one-way ANOVA: $F_{(3,20)} = 9.735$, $P = 0.000$; *post hoc* Bonferroni multiple comparison tests: hM3Dq + CNO *vs* EGFP + CNO $P = 0.001$, hM3Dq + CNO *vs* hM3Dq + vehicle $P = 0.003$; all groups $n = 6$ rats; Fig. 8B) and mechanical threshold (one-way ANOVA: $F_{(3,20)} = 29.229$, $P = 0.000$; *post hoc* Bonferroni multiple comparison tests: hM3Dq + CNO *vs* EGFP + CNO $P = 0.000$, hM3Dq + CNO *vs* hM3Dq + vehicle $P = 0.000$; all groups $n = 6$ rats; Fig. 8C). However, when the D2R antagonist (sulpiride, 50 μmol/L), but not the D1R antagonist (SCH23390, 50 μmol/L), was pre-injected into the LEC, the analgesic effect of CNO was significantly weakened, suggesting a mediating role of D2R (thermal latency: one-way ANOVA: $F_{(3,20)} = 5.576$, $P = 0.006$; *post hoc* Bonferroni multiple comparison tests: sulpi + CNO *vs* CNO $P = 0.014$, SCH + CNO *vs* CNO $P = 1.000$; mechanical threshold: one-way ANOVA: $F_{(3,20)} = 14.046$, $P = 0.000$; *post hoc* Bonferroni multiple comparison tests: sulpi + CNO *vs* CNO $P = 0.011$, SCH + CNO *vs* CNO $P = 1.000$; all groups $n = 6$ rats; Fig. 8D, E).

Finally, we tested whether the selective activation of D2Rs in LEC fan cells changes the behavioral hypersensitivity induced by intraplantar CFA injection. We directly injected 10 μmol/L quinpirole into the superficial layers of the LEC and found that quinpirole prominently increased both the thermal latency and mechanical threshold of the CFA-injured hindpaw when compared to either the contralateral paw or the ipsilateral paw of rats that received vehicle (veh) treatment (thermal latency: one-way ANOVA: $F_{(5,42)} = 22.603$, $P = 0.000$, *post hoc* Bonferroni test: quin left paw (L) *vs* quin right paw (R) $P = 0.014$, quin L *vs* veh L $P = 0.023$; mechanical threshold: one-way ANOVA: $F_{(5,42)} = 36.677$, $P = 0.000$, *post hoc* Bonferroni test: quin L *vs* quin R $P = 0.001$, quin L *vs* veh L $P = 0.001$; quin groups $n = 9$ rats, veh groups $n = 9$ rats; Fig. 8F). However, with pre-injection of 1 mmol/L 8-Br-cAMP 15 min before quinpirole injection, quinpirole failed to increase the pain thresholds, suggesting that this effect is specifically mediated by HCN channels in the LEC

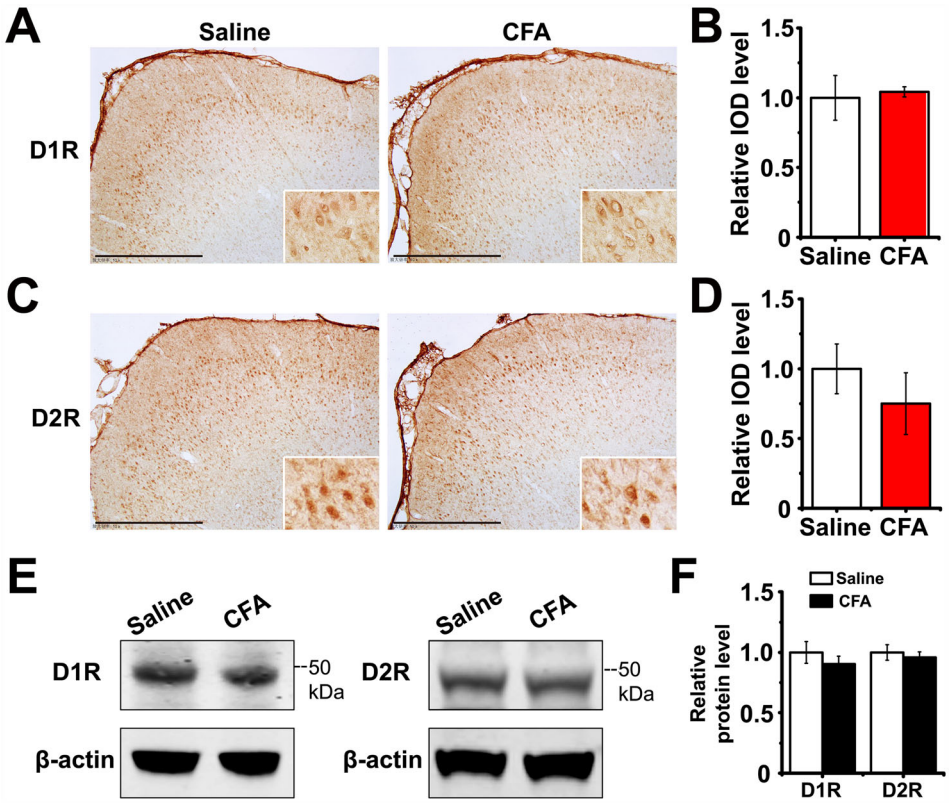

Fig. 7 The expression level of D1R and D2R in LEC do not change after CFA injection. **A** Representative immunohistochemistry images showing the expression pattern of D1R in the LEC (scale bars, 500 μm; inserts, magnified images of D1R-positive cells). **B** Relative IOD levels of D1R in the LEC are almost identical in the saline and CFA groups, as shown by immunohistochemistry. **C** Representative immunohistochemistry images showing the expression pattern of D2R in the LEC (scale bars, 500 μm; inserts, magnified images of the D2R-positive cells.) **D** Relative IOD levels of D2R in the LEC are almost identical in the saline and CFA groups, as shown by immunohistochemistry. **E** Representative images showing the protein expression of D1R and D2R in the LEC in the saline and CFA groups. **F** Western blot analysis of D1R and D2R expression levels in the saline and CFA groups.

(thermal latency: *post hoc* Bonferroni test: cAMP + quin L *vs* quin L $P = 0.026$, cAMP + quin L *vs* veh L $P = 1.000$; mechanical threshold: *post hoc* Bonferroni test: cAMP + quin L *vs* quin L $P = 0.003$, cAMP + quin L *vs* veh L $P = 1.000$; cAMP + quin groups $n = 6$ rats; Fig. 8F). These results were more clearly presented by showing the latency or threshold of the CFA-injured hindpaw as a fold decrease compared to the corresponding measures of the normal hindpaw. In this way, we also found that quinpirole significantly up-regulated the pain thresholds compared to vehicle (thermal latency: one-way ANOVA: $F_{(2,21)} = 25.121$, $P = 0.000$, *post hoc* Bonferroni test: quin *vs* veh $P = 0.000$; mechanical threshold: one-way ANOVA: $F_{(2,21)} = 19.384$, $P = 0.000$, *post hoc* Bonferroni test: quin *vs* veh $P = 0.000$), and the pre-injection of 8-Br-cAMP prevented the effect of quinpirole (thermal latency: *post hoc* Bonferroni test: cAMP + quin *vs* veh $P = 1.000$, cAMP + quin *vs* quin $P = 0.000$; mechanical threshold: *post hoc* Bonferroni test: cAMP + quin *vs* veh $P = 1.000$, cAMP + quin *vs* quin $P = 0.000$; Fig. 8G).

Discussion

Our results showed that the HCN current was up-regulated after chronic inflammatory pain, and this induced neuronal hyperexcitability in LEC fan cells. Activation of dopamine D2Rs, but not D1Rs, clearly down-regulated the I_h. In addition, the inhibitory effect of D2R on I_h was mediated by adenylate cyclase, and the indirect inhibition of the I_h through the activation of D2Rs effectively attenuated the hyperexcitability of LEC fan cells in CFA slices. Furthermore, we revealed that both activation of the VTA-LEC projection and intra-LEC activation of D2Rs alleviated CFA-evoked thermal hyperalgesia and mechanical allodynia, which were blocked by the pre-activation of the I_h.

LEC Fan Cells and Chronic Pain

The LEC-hippocampus pathway plays an important role in persistent pain. During chronic pain, there may be an increase in glutamate levels released by the terminals in the

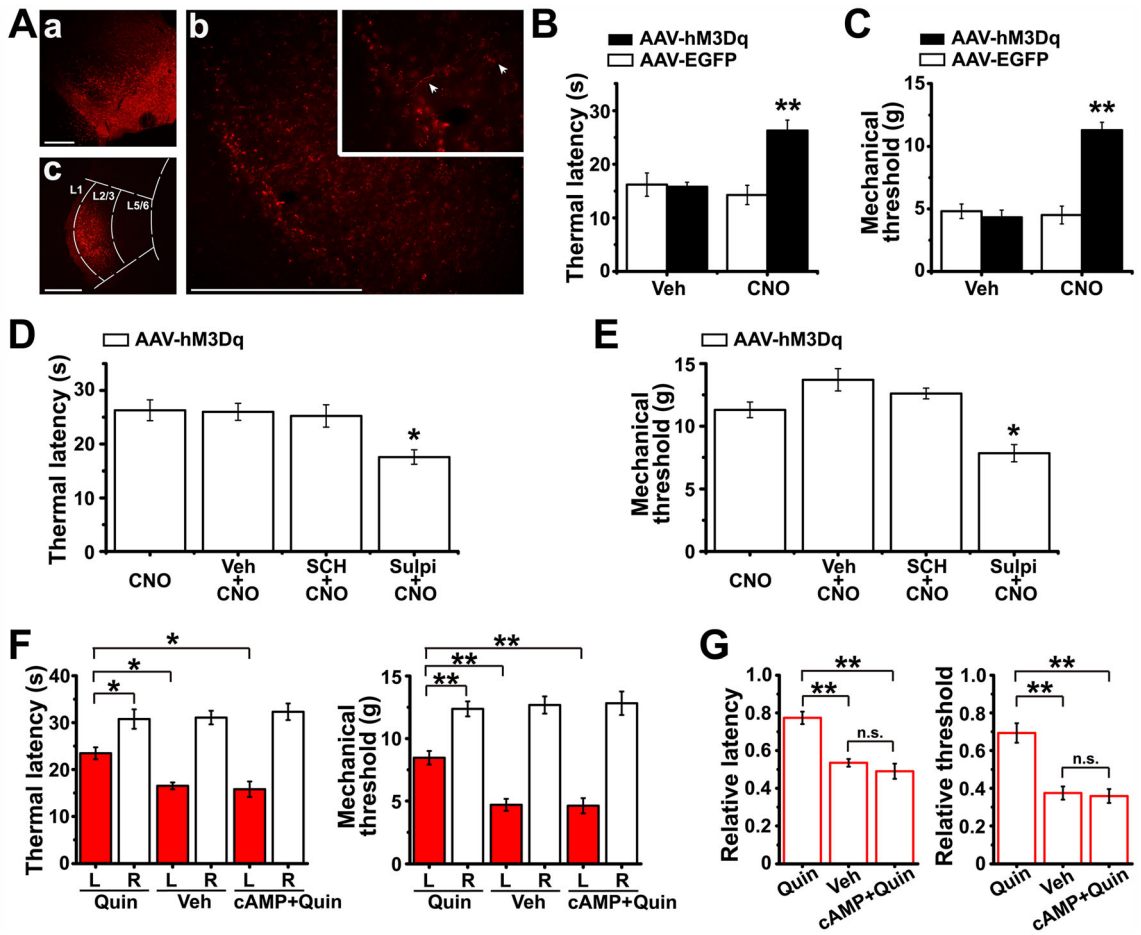

Fig. 8 Activation of VTA-LEC projection terminals or injection of quinpirole into the superficial layer of LEC alleviates behavioral hypersensitivity induced by CFA. **Aa**, Expression of AAV-hM3Dq-mCherry in the VTA 28 days after viral injection (scale bar, 500 μm). **Ab**, Expression of mCherry-positive fibers and terminals in the LEC (scale bar, 500 μm; insert, magnified image showing mCherry-positive fibers). **Ac** Histological verification of drug diffusion in the LEC (scale bar, 500 μm; L1, layer 1). **B, C** Effects of intra-LEC injection of vehicle or CNO (3 μmol/L) in AAV-hM3Dq-mCherry- or AAV-EGFP-infected CFA rats on paw withdrawal thermal latencies (**B**) and mechanical thresholds (**C**) for paws ipsilateral to the CFA injection. ** *vs* AAV-EGFP + vehicle. **D, E** Thermal latencies (**D**) and mechanical thresholds (**E**) of AAV-hM3Dq-mCherry-infected CFA rats with or without intra-LEC pre-injection of vehicle, SCH23390 (50 μmol/L), or sulpiride (50 μmol/L) before CNO application. * *vs* CNO. **F** Effect of intra-LEC injection of quinpirole, vehicle, or 8-Br-cAMP + quinpirole on thermal latency and mechanical threshold of the left and right hindpaws (CFA was injected into the left hindpaw; L, left; R, right). **G** Thermal latencies and mechanical thresholds of CFA-injured paws, normalized to the non-injured paws, in rats receiving quinpirole, vehicle, or 8-Br-cAMP + quinpirole injection. *$P < 0.05$, **$P < 0.01$; n.s., not significant.

lateral perforant pathway in the DG [41]; this has been proposed as a crucial mechanism underlying chronic neuropathic pain [42]. The fan cells, which are layer II neurons in the LEC projecting to granule cells of the DG, are the main neurons constituting the lateral perforant pathway inputs [6].

In the present study, we found that LEC fan cells showed an enhanced firing response to subthreshold depolarization, suggesting that subthreshold current injection leads to an excessive AP burst in CFA rats. Moreover, the hyperexcitable firing patterns recorded around the onset (f_o in Fig. 2F) of more prolonged suprathreshold current stimuli most likely imply that *in vivo* suprathreshold presynaptic inputs drive increases in postsynaptic firing of LEC fan cells in CFA rats. This suggestion is supported by the findings that the stimuli that usually drive AP firing in the intact brain are glutamatergic excitatory postsynaptic potentials, which exhibit a rapid rise and exponential decay over tens of milliseconds [43]. Therefore, hyperexcitable fan cells lead to more glutamate release in the DG during chronic pain.

More importantly, it has been revealed that long-term potentiation (LTP) in the LEC-DG pathway is impaired during chronic pain [2, 41]. This loss in LTP induction is associated with a higher basal amplitude and slope in response to a single pulse, possibly due to the increase in glutamate concentration in the DG [2]. Thus, our present results provide strong support for this hypothesis.

Role of Cortical I_h in Chronic Pain

Numerous studies have explored the role of cortical I_h in chronic pain. Our previous study showed that reductions in the I_h contribute to the neuronal hyperexcitability of layer V pyramidal neurons in the anterior cingulate cortex and lead to behavioral hypersensitivity during chronic neuropathic pain [8], consistent with a report by Santello and Nevian [10]. However, Koga *et al.* [9] showed that inhibition of presynaptic HCN channels at layer II/III synapses in the anterior cingulate cortex reverses chronic pain-triggered anxiety-like behaviors, exhibiting a therapeutic effect. This discrepancy suggests that the different cellular and subcellular localizations of HCN channels lead to diverse pathological functions under chronic pain conditions.

It is known that both medial entorhinal cortex (MEC) stellate cells and LEC fan cells display the I_h on the soma [44, 45]. It is also known that in rodent ECs, the size of the I_h in stellate cells is greater than that in fan cells [6, 46], which could account for the increased firing frequency of stellate cells [47]. However, little is known about the role of the I_h in the LEC during chronic pain. In the present study, we confirmed that the I_h of fan cells in CFA rats was higher than that in control rats, which accounts for the increased firing frequency of fan cells after CFA injection. Since the I_h is a nonselective inward cationic current that generates slow and non-inactivating membrane depolarization, the larger inward rectification during prolonged hyperpolarization caused by a higher I_h (Fig. 3A) could contribute to increased spike frequency in the fan cells of CFA rats [27, 47]. Given the unchanged expression of HCN1 protein, the up-regulation of I_h is probably due to altered channel activity in CFA rats, and further studies on how the I_h is up-regulated are needed.

Dopaminergic Modulation of Chronic Pain at the Cortical Level

Studies on the administration of dopaminergic drugs to control chronic pain, with a focus on increasing low dopamine levels in the mesolimbic system, have shown that it is effective [48]. Moreover, phasic activation of dopaminergic inputs from the ventral tegmental area into the medial prefrontal cortex (mPFC) reduces mechanical hypersensitivity [49]. Thus, we suggested that activation of dopamine receptors, which mimics the re-strengthening of dopaminergic innervation, would down-regulate the excitability of LEC fan cells and alleviate chronic inflammatory pain. Our present results showed that activation of D2Rs effectively down-regulated the excitability of fan cells, while activation of D1Rs had the opposite effect. This is reasonable since previous studies have shown that activation of D1Rs facilitates synaptic transmission in fan cells, while activation of D2Rs suppresses excitatory synaptic responses [22, 50, 51]. Previous research has indicated that, under normal conditions, rewarding brain stimulation leads to phasic increases in dopamine in the entorhinal cortex, resulting in D2R-dependent suppression of excitatory synaptic responses [52]. However, when the dopamine concentration is much lower, D1Rs are preferentially activated, and synaptic responses are enhanced [51]. We speculate that a similar phenomenon appears during chronic pain.

In the present study, we also explored the mechanism underlying the effects of D2Rs on cellular excitability. The results showed that activation of D2Rs inhibited adenylate cyclase, thus down-regulating the I_h and the excitability of fan cells. This is supported by the fact that D2Rs are G_i-coupled receptors and that stimulation of these receptors acts in part to inhibit adenylyl cyclase activity [53, 54]. Similarly, activation of D1Rs dramatically activates adenylate cyclase and increases the I_h [14], which again illustrates the opposing effects of D1Rs and D2Rs. In addition, chemogenetic activation of the VTA-LEC projection alleviated CFA-evoked thermal hyperalgesia and mechanical allodynia in a D2R-dependent manner, and direct activation of D2Rs by intra-LEC microinjections of a specific agonist also had an analgesic effect. This indicates that the D2R may be a potential therapeutic target for chronic inflammatory pain, just as D2R has been considered the most often used target in the dopamine receptor family for pharmacological treatments [55]. Moreover, the effect of D2R activation was blocked by pretreatment with 8-Br-cAMP at the same site, suggesting a causal relationship between D2R activation and the analgesic effects mediated by the I_h.

However, we cannot exclude the possibility that the analgesic effects in the CFA rats may have been mediated by the effects of D2R activation on other cell types in the LEC, such as pyramidal neurons in the superficial layers. Our results show that the effect of D2R is mediated by I_h to a considerable extent. Given that the I_h in fan cells is 5.26–6.79 times larger than that in pyramidal neurons [56], we speculate that the analgesic effect of D2R activation is mainly mediated by the fan cells. Nonetheless, we have not completely ruled out the possible role of pyramidal neurons. We did not explore the potential effects of dopaminergic modulation in deep layers of the LEC either. Therefore, it is crucial to identify specific effects of CFA injection and dopaminergic modulation on the different LEC neuronal subtypes in the future.

In conclusion, we provide direct evidence to support the hypothesis that D2Rs play an important role in modulating cortical pain processing in a CFA rat model. The results show that activation of D2Rs and subsequent inhibition of

adenylate cyclase are important causes of inhibition of the I_h in LEC fan cells after CFA injection. This is perhaps a novel strategy to alleviate neuronal hyperexcitability, and it, at least in part, provides new therapeutic avenues for the treatment of chronic inflammatory pain.

Acknowledgements This work was supported by the National Natural Science Foundation of China (81901119 and 81901142), Special Project on Innovation and Generation of Medical Support Capacity, and the Natural Science Foundation of Tibet (XZ2019ZRG-119), China.

Conflict of interest The authors declare that they have no competing interests.

References

1. Zhang Y, Liu FY, Liao FF, Wan Y, Yi M. Exacerbation of tonic but not phasic pain by entorhinal cortex lesions. Neurosci Lett 2014, 581: 137–142.
2. Boccella S, Cristiano C, Romano R, Iannotta M, Belardo C, Farina A. Ultra-micronized palmitoylethanolamide rescues the cognitive decline-associated loss of neural plasticity in the neuropathic mouse entorhinal cortex-dentate gyrus pathway. Neurobiol Dis 2019, 121: 106–119.
3. Bush D, Barry C, Burgess N. What do grid cells contribute to place cell firing? Trends Neurosci 2014, 37: 136–145.
4. Liu MG, Lu D, Wang Y, Chen XF, Li Z, Xu Y, *et al*. Counteracting roles of metabotropic glutamate receptor subtypes 1 and 5 in regulation of pain-related spatial and temporal synaptic plasticity in rat entorhinal-hippocampal pathways. Neurosci Lett 2012, 507: 38–42.
5. Malheiros JM, Guinsburg R, Covolan L. Cortical modulation of pain: Comments on "Exacerbation of tonic but not phasic pain by entorhinal cortex lesions." Neurosci Lett 2014, 581: 135–136.
6. Tahvildari B, Alonso A. Morphological and electrophysiological properties of lateral entorhinal cortex layers II and III principal neurons. J Comp Neurol 2005, 491: 123–140.
7. Notomi T, Shigemoto R. Immunohistochemical localization of I_h channel subunits, HCN1–4, in the rat brain. J Comp Neurol 2004, 471: 241–276.
8. Gao SH, Wen HZ, Shen LL, Zhao YD, Ruan HZ. Activation of mGluR1 contributes to neuronal hyperexcitability in the rat anterior cingulate cortex *via* inhibition of HCN channels. Neuropharmacology 2016, 105: 361–377.
9. Koga K, Descalzi G, Chen T, Ko HG, Lu JS, Li S, *et al*. Coexistence of two forms of LTP in ACC provides a synaptic mechanism for the interactions between anxiety and chronic pain. Neuron 2015, 86: 1109.
10. Santello M, Nevian T. Dysfunction of cortical dendritic integration in neuropathic pain reversed by serotoninergic neuromodulation. Neuron 2015, 86: 233–246.
11. Cordeiro Matos S, Zhang ZZ, Séguéla P. Peripheral neuropathy induces HCN channel dysfunction in pyramidal neurons of the medial prefrontal cortex. J Neurosci 2015, 35: 13244–13256.
12. Nolan MF, Dudman JT, Dodson PD, Santoro B. HCN1 channels control resting and active integrative properties of stellate cells from layer II of the entorhinal cortex. J Neurosci 2007, 27: 12440–12451.
13. Fransén E, Alonso AA, Dickson CT, Magistretti J, Hasselmo ME. Ionic mechanisms in the generation of subthreshold oscillations and action potential clustering in entorhinal layer II stellate neurons. Hippocampus 2004, 14: 368–384.
14. He C, Chen F, Li B, Hu ZA. Neurophysiology of HCN channels: From cellular functions to multiple regulations. Prog Neurobiol 2014, 112: 1–23.
15. Ozaki S, Narita M, Narita M, Iino M, Sugita J, Matsumura Y, *et al*. Suppression of the morphine-induced rewarding effect in the rat with neuropathic pain: Implication of the reduction in mu-opioid receptor functions in the ventral tegmental area. J Neurochem 2002, 82: 1192–1198.
16. Taylor AMW, Murphy NP, Evans CJ, Cahill CM. Correlation between ventral striatal catecholamine content and nociceptive thresholds in neuropathic mice. J Pain 2014, 15: 878–885.
17. Serafini RA, Pryce KD, Zachariou V. The mesolimbic dopamine system in chronic pain and associated affective comorbidities. Biol Psychiatry 2020, 87: 64–73.
18. Thompson JM, Neugebauer V. Cortico-limbic pain mechanisms. Neurosci Lett 2019, 702: 15–23.
19. Baliki MN, Petre B, Torbey S, Herrmann KM, Huang LJ, Schnitzer TJ, *et al*. Corticostriatal functional connectivity predicts transition to chronic back pain. Nat Neurosci 2012, 15: 1117–1119.
20. Lee M, Manders TR, Eberle SE, Su C, D'Amour J, Yang RT, *et al*. Activation of corticostriatal circuitry relieves chronic neuropathic pain. J Neurosci 2015, 35: 5247–5259.
21. Wang HR, Hu SW, Zhang S, Song Y, Wang XY, Wang L, *et al*. KCNQ channels in the mesolimbic reward circuit regulate nociception in chronic pain in mice. Neurosci Bull 2021, 37: 597–610.
22. Glovaci I, Chapman CA. Dopamine induces release of calcium from internal stores in layer II lateral entorhinal cortex fan cells. Cell Calcium 2019, 80: 103–111.
23. Corder G, Doolen S, Donahue RR, Winter MK, Jutras BL, He Y, *et al*. Constitutive μ-opioid receptor activity leads to long-term endogenous analgesia and dependence. Science 2013, 341: 1394–1399.
24. Pan ZQ, Zhu LJ, Li YQ, Hao LY, Yin C, Yang JX, *et al*. Epigenetic modification of spinal miR-219 expression regulates chronic inflammation pain by targeting CaMKIIγ. J Neurosci 2014, 34: 9476–9483.
25. Scheff NN, Gold MS. Trafficking of Na^+/Ca^{2+} exchanger to the site of persistent inflammation in nociceptive afferents. J Neurosci 2015, 35: 8423–8432.
26. de Castro Costa M, de Sutter P, Gybels J, van Hees J. Adjuvant-induced arthritis in rats: A possible animal model of chronic pain. Pain 1981, 10: 173–185.
27. Marcantoni A, Raymond EF, Carbone E, Marie H. Firing properties of entorhinal cortex neurons and early alterations in an Alzheimer's disease transgenic model. Pflugers Arch 2014, 466: 1437–1450.
28. Gao SH, Shen LL, Wen HZ, Zhao YD, Ruan HZ. Inhibition of metabotropic glutamate receptor subtype 1 alters the excitability of the commissural pyramidal neuron in the rat anterior cingulate cortex after chronic constriction injury to the sciatic nerve. Anesthesiology 2017, 127: 515–533.
29. Simkin D, Hattori S, Ybarra N, Musial TF, Buss EW, Richter H, *et al*. Aging-related hyperexcitability in CA3 pyramidal neurons is mediated by enhanced A-type K^+ channel function and expression. J Neurosci 2015, 35: 13206–13218.
30. van Aerde KI, Feldmeyer D. Morphological and physiological characterization of pyramidal neuron subtypes in rat medial prefrontal cortex. Cereb Cortex 2015, 25: 788–805.
31. Ionov ID, Pushinskaya II, Gorev NP, Frenkel DD. Antidepressants upregulate c-Fos expression in the lateral entorhinal cortex and hippocampal dorsal subiculum: Study in rats. Brain Res Bull 2019, 153: 102–108.

32. Paxinos G, Watson C. The rat brain in stereotaxic coordinates. Academic, New York, 1998.
33. Gao SH, Shen LL, Wen HZ, Zhao YD, Chen PH, Ruan HZ. The projections from the anterior cingulate cortex to the nucleus accumbens and ventral tegmental area contribute to neuropathic pain-evoked aversion in rats. Neurobiol Dis 2020, 140: 104862.
34. Hargreaves K, Dubner R, Brown F, Flores C, Joris J. A new and sensitive method for measuring thermal nociception in cutaneous hyperalgesia. Pain 1988, 32: 77–88.
35. Chaplan SR, Bach FW, Pogrel JW, Chung JM, Yaksh TL. Quantitative assessment of tactile allodynia in the rat paw. J Neurosci Methods 1994, 53: 55–63.
36. Kimm T, Khaliq ZM, Bean BP. Differential regulation of action potential shape and burst-frequency firing by BK and Kv2 channels in substantia nigra dopaminergic neurons. J Neurosci 2015, 35: 16404–16417.
37. Missale C, Nash SR, Robinson SW, Jaber M, Caron MG. Dopamine receptors: From structure to function. Physiol Rev 1998, 78: 189–225.
38. Mishra A, Singh S, Shukla S. Physiological and functional basis of dopamine receptors and their role in neurogenesis: Possible implication for Parkinson's disease. J Exp Neurosci 2018, 12: 1179069518779829.
39. Li B, Chen F, Ye JN, Chen XW, Yan J, Li Y, *et al*. The modulation of orexin A on HCN currents of pyramidal neurons in mouse prelimbic cortex. Cereb Cortex 2010, 20: 1756–1767.
40. Borsook D, Linnman C, Faria V, Strassman AM, Becerra L, Elman I. Reward deficiency and anti-reward in pain chronification. Neurosci Biobehav Rev 2016, 68: 282–297.
41. Boccella S, Guida F, Iannotta M, Iannotti FA, Infantino R, Ricciardi F, *et al*. 2-Pentadecyl-2-oxazoline ameliorates memory impairment and depression-like behaviour in neuropathic mice: Possible role of adrenergic alpha2- and H3 histamine autoreceptors. Mol Brain 2021, 14: 28.
42. Chung G, Kim CY, Yun YC, Yoon SH, Kim MH, Kim YK, *et al*. Upregulation of prefrontal metabotropic glutamate receptor 5 mediates neuropathic pain and negative mood symptoms after spinal nerve injury in rats. Sci Rep 2017, 7: 9743.
43. Brown JT, Chin J, Leiser SC, Pangalos MN, Randall AD. Altered intrinsic neuronal excitability and reduced Na^+ currents in a mouse model of Alzheimer's disease. Neurobiol Aging 2011, 32: 2109.e1-2109.14.
44. Alonso A, Klink R. Differential electroresponsiveness of stellate and pyramidal-like cells of medial entorhinal cortex layer II. J Neurophysiol 1993, 70: 128–143.
45. Dickson CT, Magistretti J, Shalinsky MH, Fransén E, Hasselmo ME, Alonso A. Properties and role of I_h in the pacing of subthreshold oscillations in entorhinal cortex layer II neurons. J Neurophysiol 2000, 83: 2562–2579.
46. Wang X, Lambert NA. Membrane properties of identified lateral and medial perforant pathway projection neurons. Neuroscience 2003, 117: 485–492.
47. Solomon JS, Nerbonne JM. Two kinetically distinct components of hyperpolarization-activated current in rat superior colliculus-projecting neurons. J Physiol 1993, 469: 291–313.
48. Yang S, Boudier-Revéret M, Choo YJ, Chang MC. Association between chronic pain and alterations in the mesolimbic dopaminergic system. Brain Sci 2020, 10: 701.
49. Huang S, Zhang ZZ, Gambeta E, Xu SC, Thomas C, Godfrey N, *et al*. Dopamine inputs from the ventral tegmental area into the medial prefrontal cortex modulate neuropathic pain-associated behaviors in mice. Cell Rep 2020, 31: 107812.
50. Glovaci I, Caruana DA, Chapman CA. Dopaminergic enhancement of excitatory synaptic transmission in layer II entorhinal neurons is dependent on D_1-like receptor-mediated signaling. Neuroscience 2014, 258: 74–83.
51. Caruana DA, Sorge RE, Stewart J, Chapman CA. Dopamine has bidirectional effects on synaptic responses to cortical inputs in layer II of the lateral entorhinal cortex. J Neurophysiol 2006, 96: 3006–3015.
52. Hutter JA, Martel A, Trigiani L, Barrett SG, Chapman CA. Rewarding stimulation of the lateral hypothalamus induces a dopamine-dependent suppression of synaptic responses in the entorhinal cortex. Behav Brain Res 2013, 252: 266–274.
53. Liu K, Steketee JD. The role of adenylyl cyclase in the medial prefrontal cortex in cocaine-induced behavioral sensitization in rats. Neuropharmacology 2016, 111: 70–77.
54. Vortherms TA, Nguyen CH, Bastepe M, Jüppner H, Watts VJ. D2 dopamine receptor-induced sensitization of adenylyl cyclase type 1 is Gαs independent. Neuropharmacology 2006, 50: 576–584.
55. Quintana C, Beaulieu JM. A fresh look at cortical dopamine D2 receptor expressing neurons. Pharmacol Res 2019, 139: 440–445.
56. He C, Luo FL, Chen XS, Chen F, Li C, Ren SC, *et al*. Superficial layer-specific histaminergic modulation of medial entorhinal cortex required for spatial learning. Cereb Cortex 2016, 26: 1590–1608.